# PinX1-Induced Autophagy Inhibits Cell Proliferation and Induces Cell Apoptosis by Inhibiting the NF-κB/p65 Signaling Pathway in Nasopharyngeal Carcinoma

**Mengxue Yang**
Zhujiang Hospital
**Fang Chen**
Guangzhou Red Cross Hospital https://orcid.org/0000-0001-7097-3359
**Chaosheng Yu**
Guangzhou Red Cross Hospital
**Zhimou Cai**
Zhujiang Hospital
**Qingwen Zhong**
Zhujiang Hospital
**Jialian Feng**
Zhujiang Hospital
**Guanxue Li**
Zhujiang Hospital
**Congxiang Shen**
Zhujiang Hospital
**Zhong Wen** ( wenzhong60@163.com )
https://orcid.org/0000-0003-3591-3523

**Research**

**Keywords:** Nasopharyngeal carcinoma, PinX1, Autophagy, AKT/mTOR pathway, NF-κB/p65

**Posted Date:** May 5th, 2021

**DOI:** https://doi.org/10.21203/rs.3.rs-453969/v1

# Abstract

Background

The role of PinX1 in tumorigenesis and development has been extensively studied. We have previously reported roles for PinX1 in modulating proliferation, apoptosis, EMT, and stemness in NPC cells. However, the relationship between PinX1, autophagy, and cell function in NPC remains unclear. The aim of this study was to explore the mechanisms by which PinX1 regulates autophagy in NPC, and to investigate its clinical significance and biological role with respect to disease progression.

Methods

MTT and xenograft tumorigenicity assays were used to assess the proliferative capacity of NPC cells. Autophagic flux was monitored using a tandem monomeric DAPI–FITC–LC3 reporter assay. The rates of apoptosis and the cell cycle in NPC cells were analyzed using flow cytometry. Reverse-transcription quantitative PCR was used to evaluate the expression of hTERT and PinX1. Western blot analysis was used to evaluate the activation of autophagy and the signaling status of the AKT/mTOR and NF-κB/p65 pathways.

Results

PinX1 overexpression induced autophagy and apoptosis, while suppressing NPC cell proliferation, migration, and invasion, and decelerated cell-cycle progression; inhibiting autophagy via 3-methyladenine reversed these outcomes. Mechanistic investigations clarified that PinX1 overexpression significantly reduced the expression of p-AKT, p-mTOR, p65, and p-p65. Chloroquine treatment in PinX1-overexpressing cells did not significantly alter p-AKT and p-mTOR levels, whereas 3-MA treatment in PinX1-overexpressing cells resulted in increased p65 and p-p65 expression, relative to untreated PinX1-overexpressing cells.

Conclusion

These findings indicate that PinX1 promotes autophagy by inhibiting the AKT/mTOR signaling pathway; this, in turn, inhibits the NF-κB/p65 signaling pathway, thereby inhibiting cell proliferation and induces cell apoptosis in NPC cells.


# Background

Nasopharyngeal carcinoma (NPC) is a highly malignant tumor, originating from the nasopharyngeal mucous membrane, which metastasizes easily throughout the body via the lymph nodes; it is common in South China and Southeast Asia[1, 2]. Patients with early-stage NPC often lack symptoms or have nonspecific symptoms. Approximately 75% of NPC patients are at an advanced stage when they first seek medical attention, and about 10% exhibit distant organ metastasis[3]. The locoregional control rate of NPC has improved significantly in the past decade following therapeutic improvements, including the

development of comprehensive treatment strategies such as intensity-modulated radiotherapy and chemotherapy, concurrent radiotherapy and chemotherapy[4], surgical treatments under nasal endoscopy[5], and PD-1 antibody immunosuppressive therapy[6-8]. However, the long-term survival rate of patients with NPC remains poor due to recurrence and/or distant metastasis[9]. Further the side-effects of atreatments used in NPC can lead to poor outcomes, especially in patients with locoregionally advanced NPC[10, 11]. Current research is therefore focused on clarifying the molecular mechanisms underlying tumor invasiveness and metastasis in NPC, and to investigate new treatment methods to improve prognosis and prolong survival in NPC patients.

Autophagy is a highly conserved cyclical degradation process, regulated by lysosomes, that is stably present in eukaryotes[12]. Abnormal or inhibited autophagy may induce various diseases[12], including cancer and neurodegeneration. Autophagy can make tumor cells more resistant to apoptosis[13]. In contrast, autophagy and apoptosis can act on cancer cells to promote their death[14]. Autophagy plays important roles in NPC cell proliferation and differentiation, and in chemo- and radioresistance[15]; it promotes both survival and apoptosis[16]. The effects of autophagy on tumor growth in NPC remain to be clarified; this lack of clarity may be due to differences in research targets or drugs investigated.

This study therefore aimed to clarify the regulation of autophagy in NPC cells, on the basis of our prior investigations. Preliminary research from our group indicates that transfecting NPC cells with *PinX1* inhibited their telomerase activity and proliferation, and significantly increased their apoptosis rate[17]. Our objective was therefore to examine how *PinX1* affects autophagy in NPC cells, and to elucidate the molecular mechanisms involved. Further, we aimed to elucidate the interaction between autophagy and apoptosis. Finally, the effect of *PinX1* on the oncogenesis of NPC was evaluated *in vivo*. This work will provide new and precise treatment strategies for NPC.

# Materials And Methods

### Cell lines and cell culture

The nasopharyngeal cancer cell lines CNE2 and 6-10B were purchased from the Beijing Concord Cell Resource Center (Beijing, China), and were cultured in RPMI-1640 (HyClone, USA) supplemented with 10% fetal bovine serum (FBS, Hyclone), 100 U/mL streptomycin, and 100 U/mL penicillin, in a humidified incubator with 5% $CO_2$ at 37 °C. The culture medium was replaced after 24 h, and cells were passaged after 72 h. The third passage of nasopharyngeal cancer cell lines, at the logarithmic phase of growth, were used for further experiments.

### Cell transfection and grouping

The PinX1-overexpression plasmid (pcDNA3.0-PinX1) and the empty plasmid were constructed by Guangzhou Vipotion Biotechnology Co., Ltd (Guangzhou, China). Cell transfection was conducted using Lipofectamine™ 2000 (Invitrogen, USA), according to the manufacturer's instructions. Briefly, CNE2 cells

($2 \times 10^5$ cells per well) were grown to ca. 60%–70% confluency in RPMI-1640 (HyClone) supplemented with 10% FBS (Hyclone), 100 U/mL streptomycin, and 100 U/mL penicillin, in 6-well plates (Corning Incorporated, USA), prior to transfection. Then, 16 μL of Lipofectamine™ 2000 reagent was mixed with 400 μL of Opti-MEM (Invitrogen, USA) for 10 min at room temperature. Thereafter, the mixtures were incubated with 12 μL of plasmid (20 μM) in 400 μL of Opti-MEM (Invitrogen, USA) for 15–20 min at room temperature. After the complexes of Lipofectamine™ 2000 and plasmid were formed, the mixtures were added to the CNE2 cells in each well. After culturing for 5 h, the medium was discarded and replaced with fresh medium containing 10% FBS and antibiotics. The cells were harvested after 2 d of transfection, and PinX1 expression was determined using reverse-transcription quantitative PCR (RT-qPCR) and western blotting. The cells were divided into the following groups: blank (cells without any transfection); Vector (cells transfected with the empty vector); Over-PinX1 (cells transfected with pcDNA3.0-PinX1); and Over-PinX1+3-MA (cells transfected with pcDNA3.0-PinX1 and treated with 3-methyladenine).

## MTT assay

The proliferative capacity of the transfected and non-transfected CNE2 cells was measured via MTT Assay Kit (ab211091, USA). Briefly, after culturing for 24, 48, and 72 h, the cells were seeded onto 96-well plates at $1 \times 10^5$ cells per well. MTT was added to the plates, which were then incubated for 2 h. Absorbance at 570 nm was determined using a microplate reader. The experiment was repeated three times to obtain the mean values. The cell viability curves were plotted using the culturing time as the abscissa and the OD value as the ordinate.

## Transwell assays

Migration and invasion by transfected and non-transfected CNE2 cells were determined using Transwell assays. For the migration analysis, DMEM supplemented with 10% FBS (Hyclone) was added to the lower chamber, and $2 \times 10^4$ cells in serum-free medium were added to the upper chamber. A similar protocol was used for the invasion analysis, except that the chambers were covered with Matrigel matrix (BD Biosciences, Franklin Lakes, NJ, USA). During incubation, the cells migrated and invaded through the lower membrane. Cells in the lower chambers were stained and fixed with 4% paraformaldehyde and 0.1% crystal violet, then counted under an OLYMPUS CX41 upright microscope. At least four fields of vision were randomly selected from each sample, to calculate the mean number of cells that had moved through the Matrigel, providing an index of cell invasiveness.

## Apoptosis assay

The cell-cycle phases and apoptosis rates of the transfected and non-transfected CNE2 cells were analyzed via flow cytometry, using an Annexin V/propidium iodide (PI) apoptosis detection kit (Beyotime, Shanghai, China), following the manufacturer's instructions. Briefly, after 48 h of incubation in a 96-well plate, the CNE2 cells (blank, Vector, Over-PinX1, and Over-PinX1+3-MA) were collected and stained with Annexin V-fluorescein isothiocyanate (FITC) and PI, then kept in the dark at room temperature for 15–20

min. Flow cytometry data were then acquired using a FACSCalibur HG flow cytometer (BD Biosciences). FlowJo 10 (Tree Star Software, San Carlos, CA, USA) was used to analyze the flow cytometry data.

### Reverse-transcription quantitative PCR (RT-qPCR)

Total RNA was extracted from cultured cells using TRIzol reagent (Invitrogen) following the manufacturer's instructions; it was used as a template for the reverse-transcription reactions into cDNA, following the instructions of the Bestar qPCR RT Kit (Applied Biosystems, Grand Island, NY, USA). RT-qPCR was performed using the Agilent Stratagene Mx3000 real-time qPCR Thermocycle Instrument (Agilent Stratagene, CA, USA), with the cDNA as the template and glyceraldehyde-3-phosphate dehydrogenase (*GAPDH*) as the internal reference. PCR amplifications were performed using the DBI Bestar® SybrGreen qPCR Master Mix, under these reaction conditions: pre-degeneration at 95 °C for 2 min, 40 cycles of denaturation at 94 °C for 30 s, annealing at 58 °C for 20 s, and extension at 72 °C for 20 s; and a final extension at 72 °C for 10 min. The average threshold cycle (Ct) values from three PCR assays were determined; the results were calculated based on the $2^{-\Delta\Delta Ct}$ method, and were normalized to *GAPDH* levels. Primer sequences used for qRT-PCR assays were synthesized by Shanghai Sangon Biotechnology Co., Ltd. (Shanghai, China), as follows: *PinX1* (forward: CCA GAG GAG AAC GAA ACC ACG; reverse: ACC TGC GTC TCA GAA ATG TCA); *hTERT* (forward: CCG ATT GTG AAC ATG GAC TAC G; reverse: CAC GCT GAA CAG TGC CTT C); and *GAPDH* (forward: TGT TCG TCA TGG GTG TGA AC; reverse: ATG GCA TGG ACT GTG GTC AT).

### Western blot analysis

Total protein was extracted from $1 \times 10^6$ cells using radioimmunoprecipitation assay (RIPA) lysate (Beyotime, Nanjing, China). Next, protein concentration was determined using a BCA Protein Assay Kit (Beyotime). The pretreated proteins were added to the sampling wells (each well ca. 20 μg) for protein isolation, on a 10% separation gel (120 V) and 5% spacer gel (100 V) for approximately 2 h. The protein samples were then transferred onto polyvinylidene fluoride membranes (Millipore, USA) and blocked with 5% non-fat milk for 1.5 h. Next, the membranes were washed and incubated with primary antibodies, including rabbit polyclonal anti-PinX1 (dilution, 1:1000), rabbit monoclonal anti-LC3B (dilution, 1:2000), rabbit monoclonal anti-p62 (dilution, 1:20000), rabbit monoclonal anti-Beclin-1 (dilution, 1:2000), rabbit polyclonal anti-p-AKT (dilution, 1:500), rabbit polyclonal anti-p-mTOR (dilution, 1:5000), rabbit monoclonal anti-p65 (dilution, 1:3000), mouse monoclonal anti-p-p65 (dilution, 1:5000) and rabbit monoclonal anti-GAPDH (dilution, 1:10000), at 4 °C overnight. The membranes were then washed and incubated with the horseradish peroxidase (HRP)-labeled goat anti-rabbit immunoglobulin G (IgG) secondary antibody (dilution, 1:20000, ab6721) at 37 °C for 4 h. All of these antibodies were purchased from Abcam Inc. (Cambridge, MA, USA). The target signals were visualized using an enhanced chemiluminescence detection kit (Beyotime). Densitometric analysis of the bands was carried out using the Gel imaging analysis system. Next, the Gel Doc XR imager system (Bio-Rad Laboratories, Inc., Hercules, CA, USA) was used for imaging, and Quantity One (Bio-Rad version 4.6.2) was used for

analysis. The gray value ratio of the target protein to the internal reference (GAPDH) was regarded as the relative protein expression. Experiments were repeated three times to obtain the mean values.

### Xenograft tumorigenicity assay in nude mice

Eight 4-week-old female nude mice with a body weight of 17 g were numbered randomly using earrings. A total of $1\times10^4$ logarithmically growing cells (Blank, Vector, or Over-PinX1) in 0.1 ml RPMI-1640 medium without FBS were injected subcutaneously into the right side of each nude mouse (n = 5 per group). Tumor size was measured once a week in the feeding environment. At four weeks after injection, nude mice were sacrificed and tumor grafts were isolated. The size of tumor grafts was calculated using the equation $V = (a^2*b)/2$, where $a$ is the length of short side and $b$ is the length of the long side of the tumor graft. Differences in tumor-graft volume were compared among the groups of mice injected with the three cell groups. The animals were provided by the Animal Laboratory of Southern Medical University. The *in vivo* experiments were approved by the Laboratory Animal Committee and were conducted in accordance with the National Laboratory Animal Care and Maintenance Guide.

### Immunofluorescence

CNE2 cells in each group were seeded into 6-well plates, washed with phosphate buffer solution (PBS), and fixed with 4% paraformaldehyde (PFA) at 4 °C overnight. Next, the cells were washed twice with PBS (3 min per wash), blocked with 10% goat serum for 15 min, and incubated with LC3B antibodies (dilution, 1:200) at 4°C for 1 h. After washing three times with PBS (3 min per wash), the cells were incubated with Alexa Fluor 488 conjugated secondary antibodies (dilution, 1:1000) at room temperature for 1 h. Next, the secondary antibodies were removed, and the cells were washed three times with PBS (5 min per wash). Finally, the cells were mounted with DAPI staining solution and incubated for 10 min at room temperature in the dark, and analyzed under a Bx51 inverted florescence microscope (,Olympus Corporation, Shinjuku, Japan).

### Hematoxylin-Eosin (H&E) Staining

To observe changes in tumor tissue morphology, paraffin-embedded sections of tumor tissue were stained with H&E solution. The nude mice in each group were sacrificed and their tumors were removed. The tumor tissue was then dehydrated by exposure to decreasing concentrations of ethanol, embedded in paraffin wax, and cut into sections 5 mm thick. The paraffin sections were deparaffinized then rehydrated in decreasing concentrations of ethanol, then stained with hematoxylin and eosin (both from Servicebio, Wuhan, China), following the manufacturer's protocols.

### Immunohistochemistry

Paraffin sections prepared from the *in vivo* experiments were used for immunohistochemistry assays, to detect PinX1 protein expression. The indirect streptavidin–peroxidase method was, following the manufacturer's instructions. Paraffin sections were rehydrated using Histo-Clear (National Diagnostics)

followed by a 100% to 70% ethanol gradient. Endogenous peroxidase activity was quenched using $H_2O_2$. Antigen retrieval was performed in a steamer for 30 min, in citrate antigen retrieval solution. The sections were then placed in avidin and biotin blocking solutions (Vector Labs), followed by addition of 2.5% normal horse serum (Vector Labs) and overnight incubation with rabbit polyclonal anti-PinX1 (dilution, 1:100). ImmPRESS HRP Anti-Rabbit Ig and ImmPACT DAB Peroxidase (Vector Labs) were used for detection. Detection was followed by dehydration of the tissue in a 70% to 100% ethanol gradient and in Histo-Clear, followed by mounting using Vectashield mounting medium.

### Statistical analysis

Statistical analyses were performed using SPSS 24.0 (SPSS Inc., Chicago, IL, USA). Data are expressed as the mean ± SD from at least three independent experiments. Comparisons between two groups were performed using Student's *t*-tests, one-way ANOVA for multiple groups, and a parametric generalized linear model with random effects for tumor growth and MTT assay. All statistical tests were two-sided.

## Results

### PinX1 suppresses cell growth *in vitro* and tumorigenesis *in vivo*

To identify the role of PinX1 in NPC development, we first examined its expression in the 6-10B and CNE2 cell lines. RT-qPCR and western blot analysis revealed that PinX1 was strongly expressed in 6-10B cells but weakly expressed in CNE2 cells (Fig. 1a). Therefore, the PinX1-overexpression plasmid (pcDNA3.0-PinX1) was introduced into the CNE2 cell line, to further explore its biological role in NPC. PinX1 expression was more than twofold greater in CNE2 cells treated with pcDNA3.0-PinX1 than in the blank and vector groups, based on RT-qPCR and western blot analysis (Student's *t*-tests, $P < 0.001$; Fig. 1b).

Subsequently, we examined the effect of PinX1 expression on hTERT expression and NPC cell growth *in vitro*. hTERT expression in CNE2 cells treated with pcDNA3.0-PinX1 was significantly suppressed relative to that in the blank and vector groups, based on RT-qPCR (Student's *t*-tests, $P < 0.001$; Fig. 1c). MTT assay revealed that PinX1-overexpression significantly suppressed cell growth ($P < 0.001$; Fig. 1d). These results suggest that PinX1 substantially inhibits the growth of NPC cells by targeting telomerase.

Next, we conducted an *in vivo* tumor-formation experiment, by subcutaneously injecting CNE2 cells (untreated, treated with the empty vector, or pcDNA3.0-PinX1-transfected cells) into the nude mice. The tumor growth curve was obtained by calculating the volume of tumors in each group at 7, 14, 21, and 28 days after inoculation: the tumor growth rate in the PinX1-overexpressing mice was significantly lower than that in the blank and vector groups (Fig. 2a). At 28 d after implantation, the PinX1-overexpressing mice had smaller tumor burdens (Fig. 2b) and displayed higher PinX1 expression in tumor tissues than the controls, and their transplanted tumor tissues showed fewer obviously pathological mitotic cell nuclei and cellular atypia than the control groups (Fig. 2c). These results suggest that PinX1 significantly inhibits tumorigenesis *in vivo*.

## Overexpression of PinX1 induces autophagy in NPC cells via the AKT/mTOR signaling pathway

To investigate the impact of PinX1 overexpression on autophagy, we first took advantage of the DAPI–FITC–LC3 reporter, to monitor the effect of PinX1 on autophagic flux. PinX1-overexpressing CNE2 cells contained more blue-green puncta than the control groups, suggesting that PinX1-overexpression activated autophagy (Fig. 3a). To establish whether autophagy was indeed activated in PinX1-overexpressing cells, the level of the autophagy marker, Beclin-1, was measured using western blotting. Beclin-1 protein levels were markedly elevated in PinX1-overexpressing cells, which also exhibited an elevated LC3-II/LC3-I protein ratio. In addition, p62 protein levels were reduced in PinX1-overexpressing cells, relative to the controls (Fig. 3b). Together, these observations suggest that PinX1 overexpression induces autophagy. To further investigate the role of PinX1 overexpression in cell invasion and migration, we inhibited autophagy pharmacologically using 3-MA, a widely used specific inhibitor of autophagy[18], and monitored its effects on autophagy. By monitoring autophagic flux using the DAPI–FITC–LC3 reporter, we found that 3-MA treatment of PinX1-overexpressing cells reduced the number of blue-green puncta (Fig. 3a). Western blot analysis revealed that 3-MA reduced the LC3-II/LC3-I ratio, and abolished the PinX1-overexpression-induced reduction of p62 expression (Fig. 3b). These results indicate that 3-MA is a potent inhibitor of PinX1-overexpression-induced autophagy in CNE2 cells. We then assessed the number of migrating and invading cells using the Transwell assay. This analysis showed that migration and invasion by PinX1-overexpressing cells was significantly reduced relative to the controls, while treatment with 3-MA markedly increased the number of migrating and invading PinX1-overexpressing cells (Fig. 3c).

We next investigated the mechanism whereby PinX1 overexpression activates autophagy in NPC cells. It has been reported that inhibiting the AKT/mTOR signaling pathway potently induces autophagy[29]. Therefore, we examined the state of AKT/mTOR signaling in CNE2 cells, by measuring the changes in the levels of phosphorylated AKT and mTOR: these were significantly lower in PinX1-overexpressing CNE2 cells than in the controls (Fig. 3d), indicating suppressed AKT/mTOR signaling in these cells. Adding chloroquine to PinX1-overexpressing cells did not cause significant differences in the levels of phosphorylated AKT and mTOR, relative to the untreated PinX1-overexpressing cells, although it did inhibit autophagic flux, as revealed by the immunofluorescence assay (Fig. 3e), indicating that PinX1 might directly modulate AKT phosphorylation. Together, these results suggest a mechanism whereby PinX1 overexpression inhibits the activation of AKT/mTOR signaling, thereby activating autophagy in NPC cells.

## Autophagy inhibitor 3-MA reverses the effects of PinX1 overexpression on cell proliferation, apoptosis, and the cell cycle in NPC cells

To establish whether the inhibition of cell proliferation and apoptosis induced by PinX1 overexpression is caused by the induction of autophagy, we used 3-MA to block autophagy, and investigated its effect on these processes in PinX1-overexpressing cells, using a MTT assay. Relative to the controls, the CNE2 cell proliferation was significantly inhibited by PinX1 overexpression, and this effect was reversed by treating

PinX1-overexpressing cells with 3-MA (Fig. 4a). We next investigated how inhibiting autophagy affected apoptosis in PinX1-overexpressing cells. Flow cytometry analysis revealed an obviously higher apoptosis rate in PinX1-overexpressing cells than in the control groups; further, treating PinX1-overexpressing cells with 3-MA markedly reduced the rate of apoptosis, relative to the untreated PinX1-overexpressing cells (Fig. 4b). Taken together, these results demonstrate that inhibiting autophagy reverses the inhibition of cell proliferation, and induction of apoptosis, that result from PinX1 overexpression. Furthermore, we monitored the effect of inhibiting autophagy on the cell cycle in PinX1-overexpressing cells. The percentage of cells in the G0/G1 phase was higher, and that of cells in G2/M phase was lower, in PinX1-overexpressing cells than in the control groups (Fig. 4c). Further, treating PinX1-overexpressing cells with 3-MA significantly reduced the percentage of cells in the G0/G1 phase and increased that of cells in the G2/M phase. These findings indicate that inhibiting autophagy reverses the deceleration of cell-cycle progression caused by PinX1 overexpression in CNE2 cells.

### PinX1 overexpression induces cell apoptosis by promoting autophagy, via the NF-κB/p65 signaling pathway

To further elucidate the signaling pathway involved in PinX1-overexpression-induced apoptosis, we assessed NF-κB/p65 signaling in CNE2 cells, by measuring changes in the levels of p65 and p-p65. Expression of p65 and p-p65 was significantly lower in PinX1-overexspressing CNE2 cells than in the controls (Fig. 5). In addition, 3-MA treatment of PinX1-overexpressing cells increased the expression of p65 and p-p65 relative to untreated PinX1-overexpressing cells. These results indicate that PinX1 overexpression promotes autophagy, thereby inhibiting the NF-κB/p65 signaling pathway, thus inducing apoptosis.

## Discussion

We have previously reported roles for PinX1 in modulating proliferation, apoptosis, EMT, and stemness in NPC cells[19]. Here, we investigated the mechanisms whereby PinX1 influences proliferation, apoptosis, and autophagy in NPC cells.

There is substantial evidence that PinX1, which has crucial roles in the carcinogenesis of many cancers, is a potential novel human cancer diagnostic biomarker and therapeutic target[20, 21]. Previous studies have shown that PinX1 can specifically inhibit telomerase activity and induce tumor-cell apoptosis[22, 23]. Here, we examined PinX1 expression in two NPC cell lines, CNE2 and 6-10B, using RT-qPCR and western blot analysis. Our findings showed that PinX1 was strongly expressed in 6-10B cells but weakly expressed in CNE2 cells. We therefore chose the CNE2 cell line for subsequent experiments, to clarify the roles and mechanisms of action of PinX1 in cell proliferation and tumorigenesis. Not only did PinX1 significantly inhibit NPC cell proliferation *in vitro*, it also suppressed tumorigenicity *in vivo*. These results suggest that PinX1 functions as a potential tumor suppressor in NPC.

It is well established that autophagy is involved in tumor growth, proliferation, and apoptosis[24-26]. However, it remains unclear how autophagy affects carcinogenesis in NPC; this may be related to differences in research targets. For example, Liu et al. demonstrated that TIPE1 promoted NPC progression by inducing cell proliferation and inhibiting autophagy via the AMPK/mTOR signaling pathway. Zhu et al.[27] showed that Annexin A1 promotes NPC cell invasion and metastasis by suppressing autophagy via activation of PI3K/AKT signaling. Here, we found that PinX1 overexpression significantly increased the density of characteristic autophagosomes and increased LC3B expression in NPC cells. Further, the LC3-II/LC3-I ratio, and Beclin-1 expression, were higher in PinX1-overexpressing cells than in the controls. Conversely, PinX1 overexpression downregulated p62 levels. Together, these results confirm that PinX1 overexpression induces autophagy in NPC cells. In addition, pharmacological inhibition of autophagy using 3-MA significantly reversed these outcomes in PinX1-overexpressing cells, which significantly increased the number of migrating and invading cancer cells, enhanced their proliferative capacity, and reduced apoptosis. Our data strongly suggest that PinX1 inhibits cell proliferation and induces cell apoptosis by inducing autophagy in NPC cells.

The AKT/mTOR signaling pathway is a key pathway in regulating autophagy, and plays a vital role in tumorigenesis[28-30]. It is known that p-AKT and p-mTOR are highly expressed in various NPC cell lines, and activation of the AKT/mTOR signaling pathway is closely related to poor prognosis[31, 32]. Here, PinX1 overexpression produced significantly lower levels of phosphorylated AKT and mTOR than in the control groups, suggesting that PinX1 inhibits AKT and its downstream target, mTOR. Further, adding chloroquine to PinX1-overexpressing cells inhibited autophagic flux but did not induce any significant changes in the levels of phosphorylated AKT and mTOR, relative to the untreated PinX1-overexpressing cells. Chloroquine inhibits autophagy mainly by reducing autophagosome–lysosome fusion, rather than by altering the acidity or degradation activity of organelles[49]. Therefore, chloroquine did not affect the signaling molecules that induce autophagosome formation. Our results confirm that PinX1 overexpression inhibits the activation of the AKT/mTOR pathway, thereby activating autophagy in NPC cells.

Cell-cycle progression is a predominant factor promoting tumor-cell proliferation and inducing apoptosis. Therefore, we examined the effects of PinX1 on the cell cycle. PinX1 overexpression decelerated cell-cycle progression and induced cell apoptosis by activating autophagy in CNE2 cells. Notably, activation of the NF-κB pathway is the main catalyst for the expression of anti-apoptotic genes in cells, which plays an important role in promoting tumor survival[33]. Therefore, we examined the state of NF-κB/p65 signaling in CNE2 cells, by measuring changes in the levels of p65 and p-p65, to elucidate the mechanism involved in PinX1-overexpression-induced cell apoptosis. PinX1 overexpression remarkably inhibited the NF-κB/p65 signaling pathway in CNE2 cells. Furthermore, inhibiting autophagy in PinX1-overexpressing cells remarkably rescued their p65 and p-p65 expression. These findings show that PinX1, by promoting autophagy, inhibits the NF-κB/p65 signaling pathway, thereby inducing apoptosis.

# Conclusions

Our findings show that PinX1 promotes autophagy by inhibiting the AKT/mTOR signaling pathway. This, in turn, inhibits the NF-κB/p65 signaling pathway, thereby inhibiting cell proliferation and inducing cell apoptosis in NPC cells. As these processes play a vital role in NPC malignancy in humans, our results reveal that autophagy may be a pivotal target for NPC therapy.

# Abbreviations

NPC: Nasopharyngeal carcinoma; EMT: Epithelial–mesenchymal transition; CSCs: cancer stem cells; PinX1: Pin2/telomeric repeat factor 1-interacting telomerase inhibitor 1; 3-MA: 3-methyladenine; FBS: Fetal bovine serum; FITC: fluorescein isothiocyanate; GAPDH: Glyceraldehyde-3-phosphate dehydrogenase; MTT: 3-(4,5)-dimethylthiahiazo(-z-y1)-3,5-di-phenytetrazoliumromide; hTERT: human telomerase reverse transcriptase; RT-qPCR: Reverse transcription-quantitative polymerase chain reaction; RIPA: radioimmunoprecipitation assay; H&E: Hematoxylin-Eosin; AKT: protein kinase B; mTOR: mammalian target of rapamycin.

# Declarations

### Ethics approval and consent to participate

The *in vivo* experiments were approved by the Laboratory Animal Committee and were conducted in accordance with the National Laboratory Animal Care and Maintenance Guide.

### Consent for publication

Not applicable

### Availability of data and materials

All data generated or analyzed during this study are included in this published article.

### Competing interests

The authors declare that they have no competing interests.


### Funding

This work was supported by the grants from National Natural Science Foundation of China Youth Fund (81402456) and Science and Natural Science Foundation of Guangdong province, China (2015A030313255).


### Authors' contributions

FC, CS and ZW developed the conception and design of the study. MY, FC and CY performed most of the experiments (RT-qPCR and Western blot analysis) and analyzed the data. ZC, QZ and JF performed the

cell culture and assessment of cell functions in vivo. MY, FC prepared all the figures and wrote the manuscript. GL, CS and ZW reviewed and revised the manuscript. All authors approved the final manuscript.

**Acknowledgements**

Not applicable

# References

1 Guo Y, Hao Y, Guan G, Ma S, Zhu Z, Guo F *et al*. Mukonal Inhibits Cell Proliferation, Alters Mitochondrial Membrane Potential and Induces Apoptosis and Autophagy in Human CNE1 Nasopharyngeal Carcinoma Cells. *Med. Sci. Monitor***25,** 1976-1983 (2019).

2 Wei K-R, Zheng R-S, Zhang S-W, Liang Z-H, Li Z-M, Chen W-Q. Nasopharyngeal carcinoma incidence and mortality in China, 2013. *Chin. J. Cancer***36** (2017).

3 Wu F, Wang R, Lu H, Wei B, Feng G, Li G *et al*. Concurrent chemoradiotherapy in locoregionally advanced nasopharyngeal carcinoma: Treatment outcomes of a prospective, multicentric clinical study. *Radiother. Oncol.* **112,** 106-111 (2014).

4 Ak S, Kilic C, Ozlugedik S. Correlation of PET-CT, MRI and histopathology findings in the follow-up of patients with nasopharyngeal cancer. *Brazil. J. Otorhinolaryngol.* (2020).

5 Wong EHC, Liew YT, Abu Bakar MZ, Lim EYL, Prepageran N. A preliminary report on the role of endoscopic endonasal nasopharyngectomy in recurrent rT3 and rT4 nasopharyngeal carcinoma. *Eur. Arch. Oto-Rhino-L.***274,** 275-281 (2017).

6 Lam WKJ, Chan JYK. Recent advances in the management of nasopharyngeal carcinoma. *F1000Research***7** (2018).

7 Ni X, Song Q, Cassady K, Deng R, Jin H, Zhang M *et al*. PD-L1 interacts with CD80 to regulate graft-versus-leukemia activity of donor CD8(+) T cells. *J. Clin. Invest.***127,** 1960-1977 (2017).

8 Jiang Y, Xie J, Han Z, Liu W, Xi S, Huang L *et al*. Immunomarker Support Vector Machine Classifier for Prediction of Gastric Cancer Survival and Adjuvant Chemotherapeutic Benefit. *Clin. Cancer Res.***24,** 5574-5584 (2018).

9 Lee HM, Okuda KS, Gonzalez FE, Patel V. Current Perspectives on Nasopharyngeal Carcinoma. In: Rhim JS, Dritschilo A, Kremer R (eds). *Human Cell Transformation: Advances in Cell Models for the Study of Cancer and Aging*. pp 11-34 (2019).

10 Lee AWM, Ma BBY, Ng WT, Chan ATC. Management of Nasopharyngeal Carcinoma: Current Practice and Future Perspective. *J. Clin. Oncol.***33,** 3356-+ (2015).

11 Xu T, Tang J, Gu M, Liu L, Wei W, Yang H. Recurrent nasopharyngeal carcinoma: a clinical dilemma and challenge. *Curr. Oncol.***20,** E406-E419 (2013).

12 Parzych KR, Klionsky DJ. An Overview of Autophagy: Morphology, Mechanism, and Regulation. *Antioxid. Redox Sign.* **20,** 460-473 (2014).

13 Chen K-H, Guo Y, Li L, Qu S, Zhao W, Lu Q-T *et al*. Cancer stem cell-like characteristics and telomerase activity of the nasopharyngeal carcinoma radioresistant cell line CNE-2R. *Cancer Med.* **7,** 4755-4764 (2018).

14 Zhao Y-y, Tian Y, Liu L, Zhan J-h, Hou X, Chen X *et al*. Inhibiting eEF-2 kinase-mediated autophagy enhanced the cytocidal effect of AKT inhibitor on human nasopharyngeal carcinoma. *Drug Des. Dev. Ther.***12,** 2655-2663 (2018).

15 Zheng R, Chen K, Zhang Y, Huang J, Shi F, Wu G *et al*. Apogossypolone induces apoptosis and autophagy in nasopharyngeal carcinoma cells in an in vitro and in vivo study. *Oncol. Lett.***14,** 751-757 (2017).

16 Han Y, Shi D, Li J. Inhibition of Nasopharyngeal Carcinoma by Beta-Lapachone Occurs by Targeting the Mammalian Target of Rapamycin (mTOR)/PI3K/AKT Pathway, Reactive Oxygen Species (ROS) Production, and Autophagy Induction. *Med. Sci. Monitor* **25,** 8995-9002 (2019).

17 Xiao-Fen L, Cong-Xiang S, WEN-zhong. Expression and effective analysis of telomerase inhibitor PinX1 in nasopharyngeal carcinoma cells. *Chin. J. Otorhinolaryngol. Skull Base Surg.***17,** 161-166 (2011).

18 Khan T, Relitti N, Brindisi M, Magnano S, Zisterer D, Gemma S *et al*. Autophagy modulators for the treatment of oral and esophageal squamous cell carcinomas. *Med. Res. Rev.***40,** 1002-1060 (2020).

19 Yu C, Chen F, Wang X, Cai Z, Yang M, Zhong Q *et al*. Pin2 telomeric repeat factor 1-interacting telomerase inhibitor 1 (PinX1) inhibits nasopharyngeal cancer cell stemness: implication for cancer progression and therapeutic targeting. *J. Exp. Clin. Cancer Res.***39** (2020).

20 Liang H, Xiong Z, Li Y, Kong W, Yao Z, Li R *et al*. Prognostic and Clinicopathological Value of PINX1 in Various Human Tumors: A Meta-Analysis. *Biomed Res. Int.* **2018** (2018).

21 Zuo J, Wang D-H, Zhang Y-J, Liu L, Liu F-L, Liu W. Expression and mechanism of PinX1 and telomerase activity in the carcinogenesis of esophageal epithelial cells. *Oncol. Rep.***30,** 1823-1831 (2013).

22 Fan X-K, Yan R-H, Geng X-Q, Li J-S, Chen X-M, Li J-Z. Biological significance of PinX1 telomerase inhibitor in esophageal carcinoma treatment. *Exp. Ther. Med.***12,** 2196-2200 (2016).

23 Shen C, Chen F, Wang H, Li G, Yu C, Wang X *et al*. The Pinx1 Gene Downregulates Telomerase and Inhibits Proliferation of CD133(+) Cancer Stem Cells Isolated from a Nasopharyngeal Carcinoma Cell Line by Regulating Trfs and Mad1/C-Myc/p53 Pathways. *Cell. Physiol. Biochem.***49,** 282-294 (2018).

24 Bishop E, Bradshaw TD. Autophagy modulation: a prudent approach in cancer treatment? *Cancer Chemoth. Pharm.***82,** 913-922 (2018).

25 Amaravadi R, Kimmelman AC, White E. Recent insights into the function of autophagy in cancer. *Genes Dev.***30,** 1913-1930 (2016).

26 Brech A, Ahlquist T, Lothe RA, Stenmark H. Autophagy in tumour suppression and promotion. *Mol. Oncol.***3,** 366-375 (2009).

27 Zhu J-F, Huang W, Yi H-M, Xiao T, Li J-Y, Feng J *et al*. Annexin A1-suppressed autophagy promotes nasopharyngeal carcinoma cell invasion and metastasis by PI3K/AKT signaling activation. *Cell Death Dis.***9** (2018).

28 Heras-Sandoval D, Perez-Rojas JM, Hernandez-Damian J, Pedraza-Chaverri J. The role of PI3K/AKT/mTOR pathway in the modulation of autophagy and the clearance of protein aggregates in neurodegeneration. *Cell. Signal.***26,** 2694-2701 (2014).

29 Fan C, Tang X, Ye M, Zhu G, Dai Y, Yao Z *et al*. Qi-Li-Qiang-Xin Alleviates Isoproterenol-Induced Myocardial Injury by Inhibiting Excessive Autophagy via Activating AKT/mTOR Pathway. *Front. Pharmacol.***10** (2019).

30 Murugan AK. mTOR: Role in cancer, metastasis and drug resistance. *Semin. Cancer Biol.***59,** 92-111 (2019).

31 Wang W, Wen Q, Xu L, Xie G, Li J, Luo J *et al*. Activation of Akt/mTOR Pathway Is Associated with Poor Prognosis of Nasopharyngeal Carcinoma. *Plos One***9** (2014).

32 Lin Y-T, Wang H-C, Hsu Y-C, Cho C-L, Yang M-Y, Chien C-Y. Capsaicin Induces Autophagy and Apoptosis in Human Nasopharyngeal Carcinoma Cells by Downregulating the PI3K/AKT/mTOR Pathway. *Int. J. Mol. Sci.***18** (2017).

33 Karin M. Nuclear factor-kappa B in cancer development and progression. *Nature***441,** 431-436 (2006).

# Figures

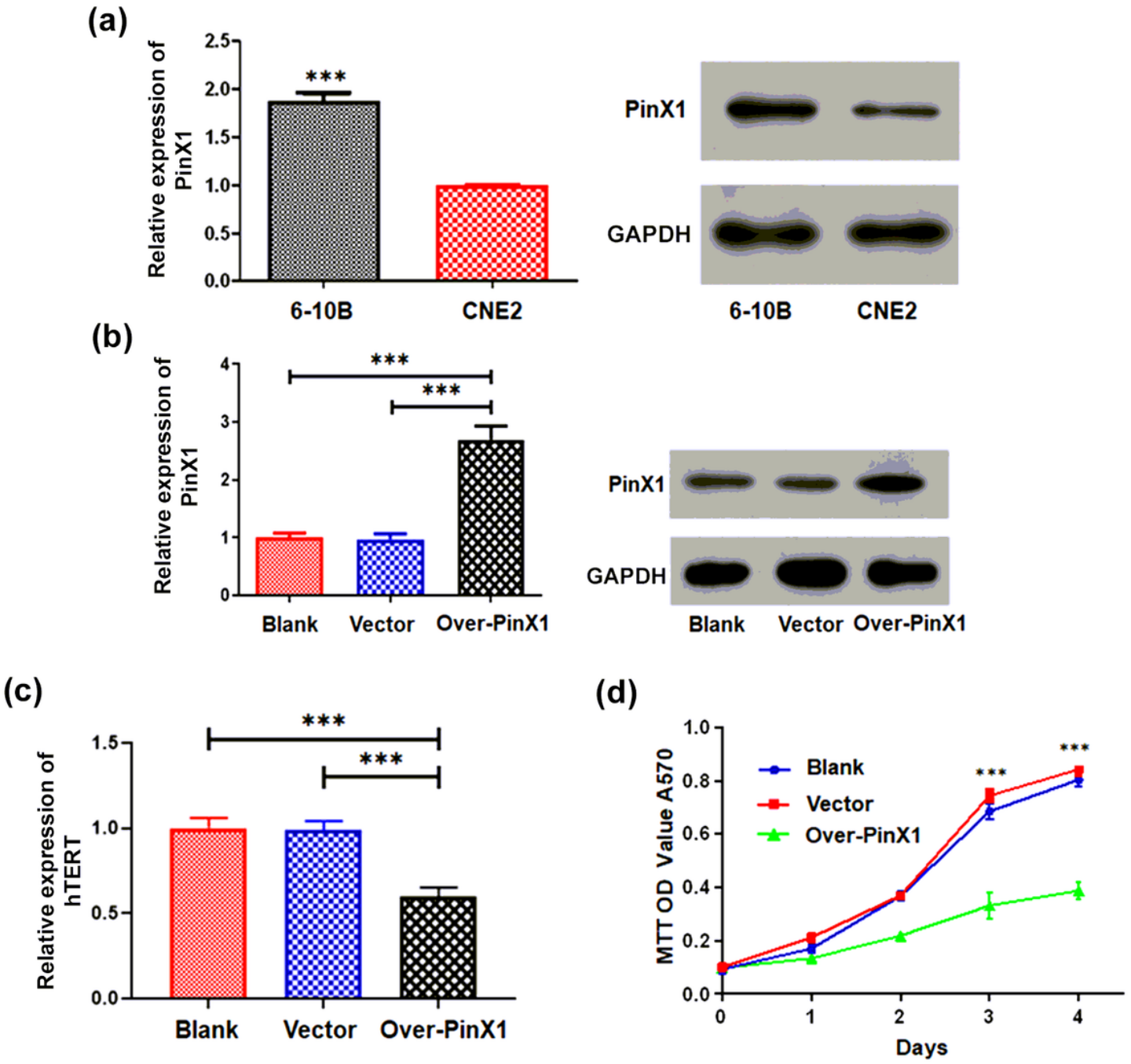


## Figure 1

PinX1 inhibits the growth of NPC cells by targeting telomerase. (a) The expressions of PinX1 in the 6-10B and CNE2 cell lines as determined by RT-qPCR and western blot analysis. (b) The expression of PinX1 in CNE2 cells and cells transfected with empty vector and pcDNA3.0-PinX1 as determined by RT-qPCR and western blot analysis. (c) The mRNA expression of hTERT in CNE2 cells and cells transfected with empty vector and pcDNA3.0-PinX1 as determined by RT-qPCR. (d) The cell proliferation curves of CNE2 cells and cells transfected with empty vector and pcDNA3.0-PinX1 was measured via MTT Assay. *** $p < 0.001$ vs. control.

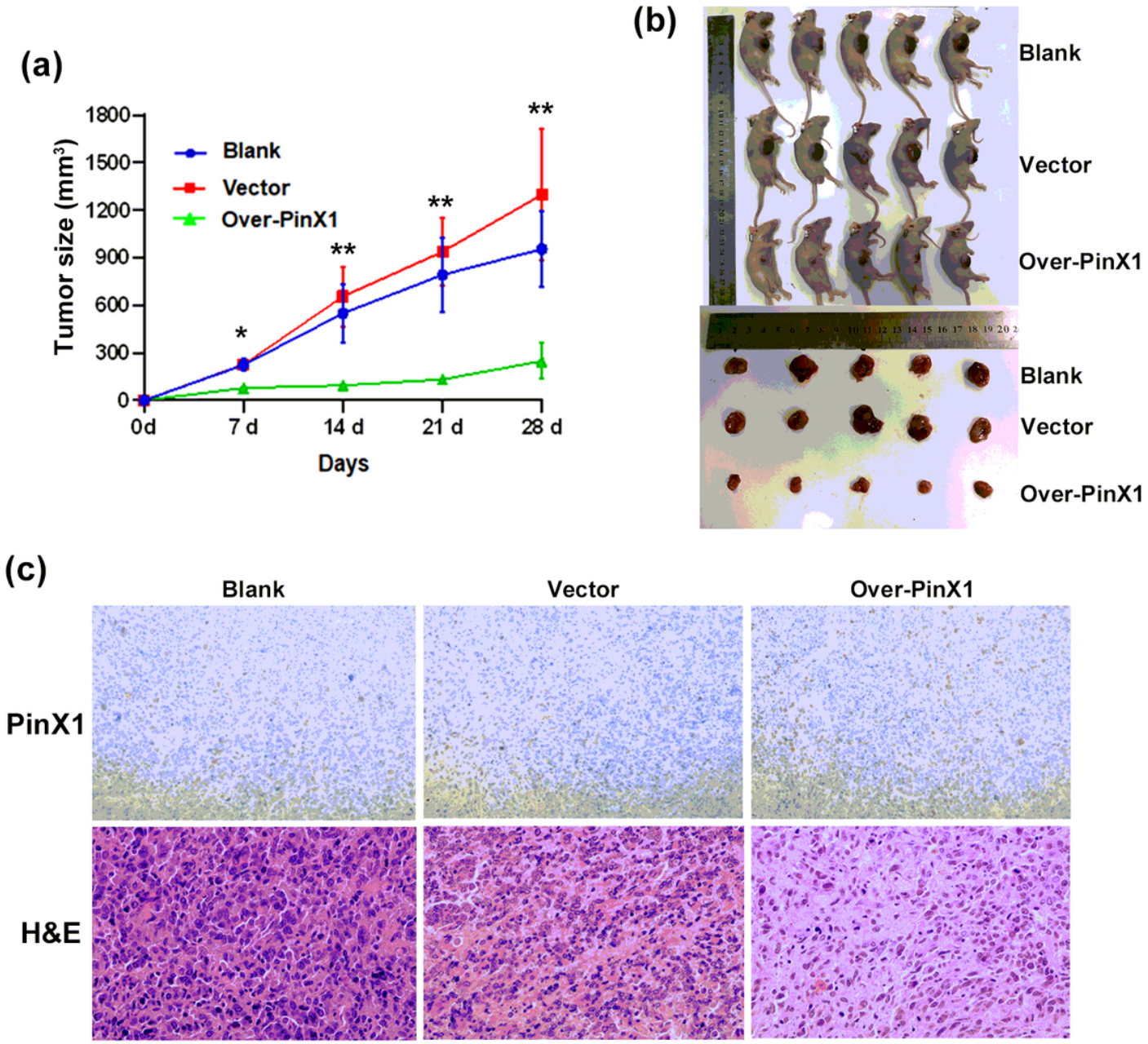


## Figure 2

PinX1 inhibits NPC tumorigenesis in vivo. (a) tumour growth curves was plotted in CNE2 cells and cells transfected with empty vector and pcDNA3.0-PinX1. (b) The xenograft mice models bearing tumours originating from CNE2 cells and cells transfected with empty vector and pcDNA3.0-PinX1 (n = 5 /group) and tumour volume was periodically measured for each mice. (c) Immunohistochemistry detection of PinX1 in xenografts derived from CNE2 cells and cells transfected with empty vector and pcDNA3.0-PinX1 as well as Representative H&E staining of primary cancer tissues are shown. Magnification ×400. Scale bar: 30 μm. * $p < 0.05$ vs. control, ** $p < 0.01$ vs. control.

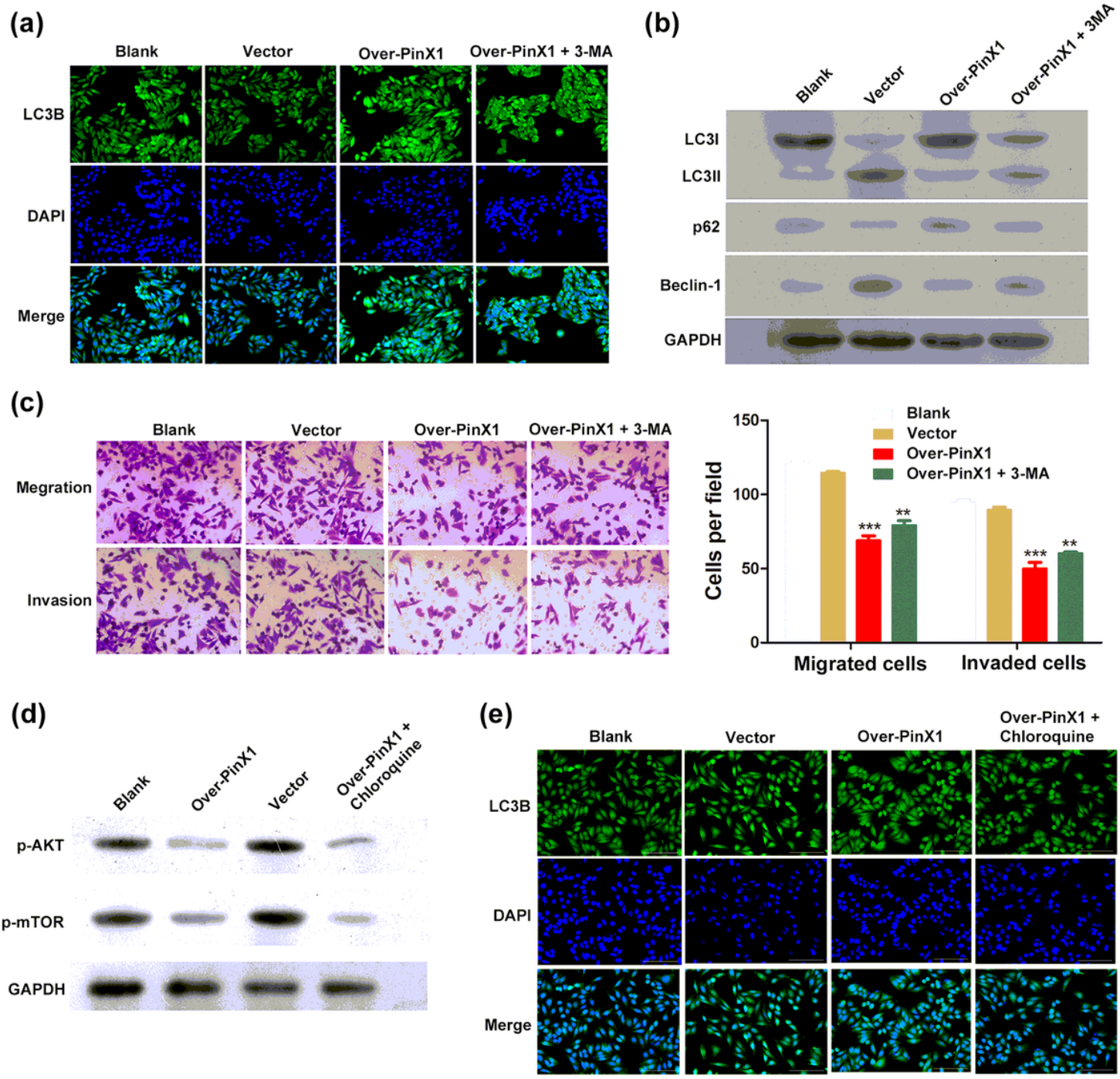


## Figure 3

Overexpression of PinX1 induces autophagy in NPC cells via the AKT/mTOR signaling pathway. (a) Comparison of autophagy flux and (b) the protein levels of LC3-II, LC3-I, p62 and Beclin-1 in CNE2 cells and cells transfected with empty vector and pcDNA3.0-PinX1 as well as pcDNA3.0-PinX1 + 3-methyladenine. (c) Cell migration and invasion following transfection as measured by Transwell assay. (d) The protein levels of p-AKT and p-mTOR and (e) Comparison of autophagy flux in CNE2 cells and cells transfected with empty vector and pcDNA3.0-PinX1 as well as pcDNA3.0-PinX1 + Chloroquine. ** $p < 0.01$ vs. control, *** $p < 0.001$ vs. control.

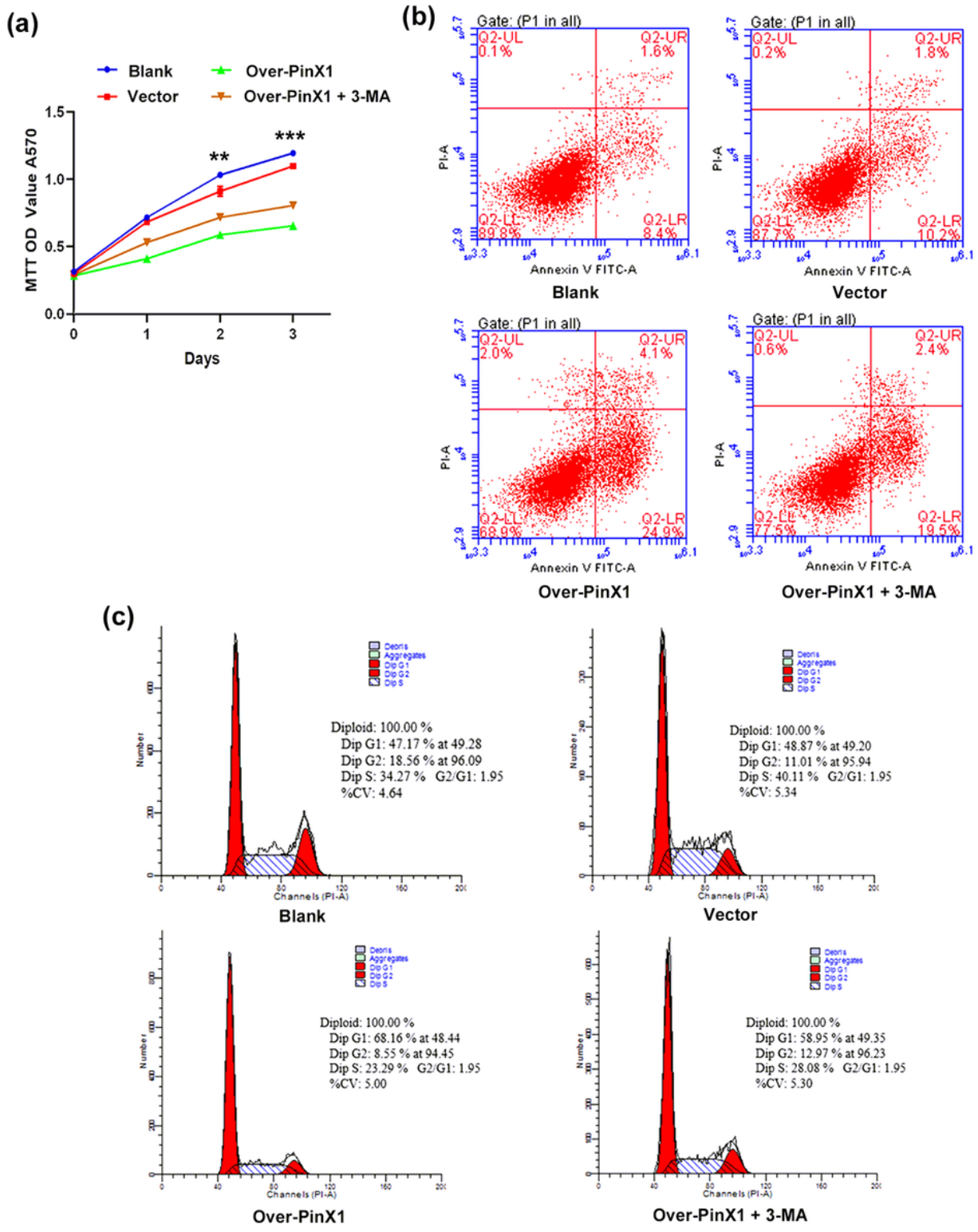


## Figure 4

Autophagy inhibitor 3-MA reverses the effects of PinX1 overexpression on cell proliferation, apoptosis, and the cell cycle in NPC cells. (a) The cell proliferation curves, (b) the apoptosis rate and (c) the cell cycle of CNE2 cells and cells transfected with empty vector and pcDNA3.0-PinX1 as well as pcDNA3.0-PinX1 + 3-methyladenine. ** $p < 0.01$ vs. control, *** $p < 0.001$ vs. control.

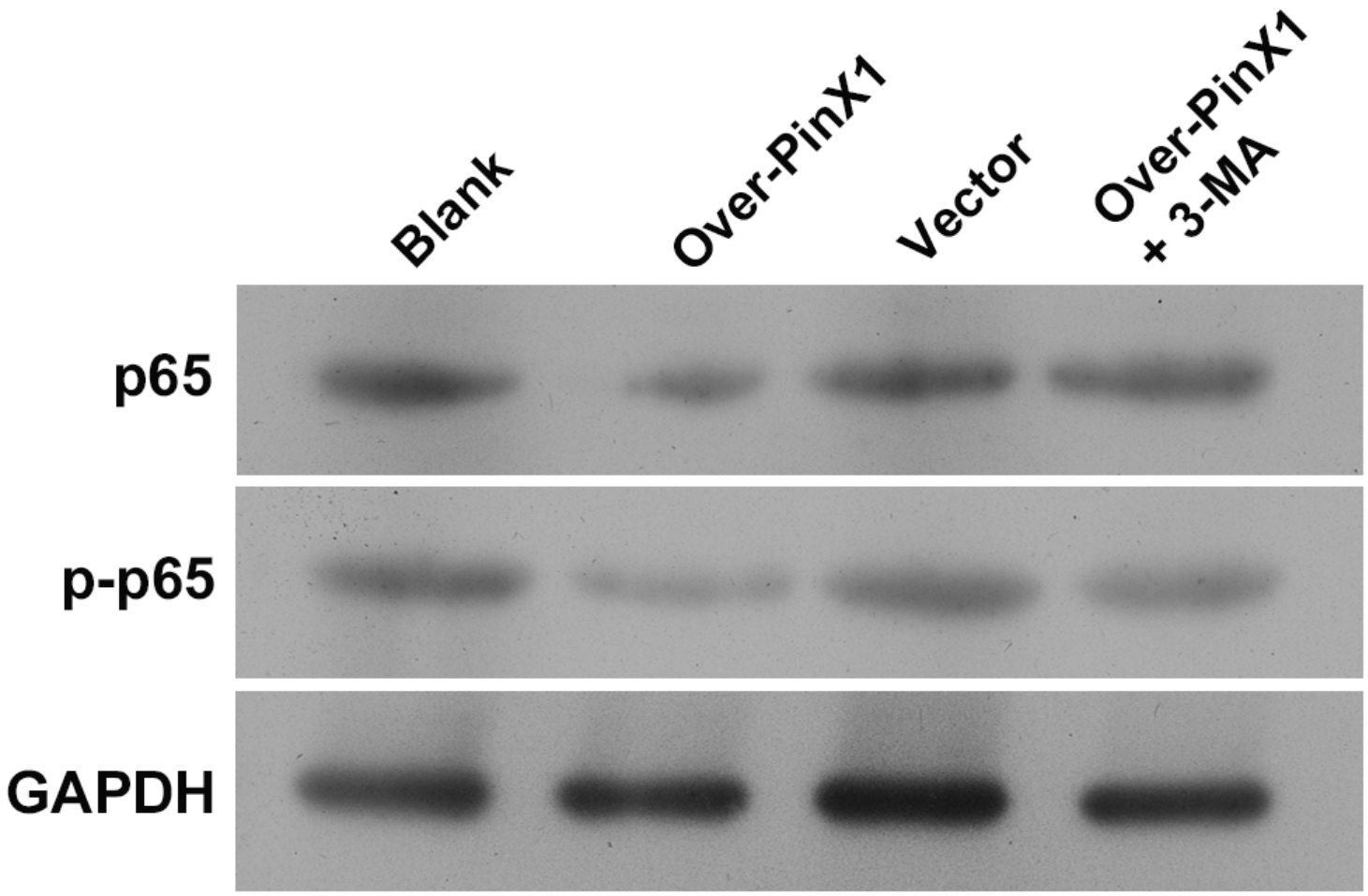


**Figure 5**

The protein levels of p65 and p-p65 in CNE2 cells and cells transfected with empty vector and pcDNA3.0-PinX1 as well as pcDNA3.0-PinX1 + 3-methyladenine as determined by Western blot.